Electronic supplementary information for:

Pasteur's Tartaramide/Malamide Quasiracemates: New Entries and Departures from Near Inversion Symmetry

Emily N. Pinter, Lee S. Cantrell, Graeme M. Day and Kraig A. Wheeler

Department of Chemistry, Whitworth University, Spokane, WA 99251, USA. E-mail: kraigwheeler@whitworth.edu; Tel: +1 509 777 3643

Electronic Supplementary Information

Table of Contents **Page**

S1. Experimental Details

General Considerations. All chemicals and solvents were purchased from the Aldrich Chemical Co. or Acros Chemicals and used as received without further purification. ^{1}H and ^{13}C NMR spectral data were recorded with a 400 MHz Bruker Avance spectrometer using TopSpin v.3.2. Spectra were referenced using the solvent residual signal as internal standard. The chemical shift values are expressed as δ values (ppm) and the value of coupling constants (*J*) in Hertz (Hz). The following abbreviations were used for signal multiplicities: s, singlet; d, doublet; dd, doublet of doublets; t, triplet; q, quartet; quin, quintet; sex, sextet; m, multiplet; and br, broad.Melting point data were determined using a Melt-Temp apparatus and are uncorrected. Recrystallization experiments were conducted at room temperature using reagent-grade solvents.

Dimethyl (2*R*,3*R*)-(+)-2,3-dihydroxybutanedioate, dimethyl (2*S*)-(-)-2-hydroxybutanedioate, dimethyl (±)-2,3-dihydroxybutanedioate, dimethyl (±)-2-hydroxybutanedioate

The procedure followed for the synthesis of the enantiopure and racemic esters was adapted from previous synthetic reports[1,2]. To a round bottom flask, the appropriate acid (L-(+)-tartaric or L-(-)-malic, 1 equivalent) was added to anhydrous methanol (20 equivalents, dried over 4 Å molecular sieves) and stirred until dissolved. Thionyl chloride (2.5 equivalents) was slowly added at 0°C and left to cool for 15 minutes before being refluxed for 2 hours. The resulting solution was reduced under *vacuo* to remove the excess methanol and then subsequently extracted with deionized water (10 mL), saturated sodium bicarbonate (10 mL), brine (10 mL), and then 8 x 10 mL of EtOAc. The combined organic extracts were dried over anhydrous $MgSO_4$ and then reduced under *vacuo* to give either pale-yellow oils or a colorless solid in 43-92% yield.

Dimethyl (2*R*,3*R*)-(+)-2,3-dihydroxybutanedioate: 62% yield. ^{1}H NMR (400MHz, $CDCl_3$): δ 4.57 (s, 2H, CH); 3.87 (s, 6H, CH_3); 3.67 (s, 2H, OH). ^{13}C NMR (100MHz, $CDCl_3$): δ 171.91, 72.03, 53.01.

Dimethyl (2*S*)-(-)-2-hydroxybutanedioate: 91% yield. ^{1}H NMR (400MHz, $CDCl_3$): δ 4.52 (dd, *J* = 4.4, 6.1 Hz, 1H, CH); 3.82 (s, 3H, CH_3); 3.72 (s, 3H, CH_3); 2.88 (dd, *J* = 4.4, 16.4 Hz, 1H, CH_2); 2.80 (dd, *J* = 6.1, 16.4 Hz, 1H, CH_2). ^{13}C NMR (100MHz, $CDCl_3$): δ 173.71, 170.98, 67.22, 52.83, 52.01, 38.41.

Dimethyl (±)-2,3-dihydroxybutanedioate: 43% yield, Mp 71-73 °C. ^{1}H NMR (400MHz, $CDCl_3$): δ 4.58 (s, 2H, CH); 3.89 (s, 6H, CH_3). ^{13}C NMR (100MHz, $CDCl_3$): δ 172.21, 72.34, 53.46.

Dimethyl (±)-2-hydroxybutanedioate: 83% yield. ^{1}H NMR (400MHz, $CDCl_3$): δ 4.52 (dd, *J* = 4.4 and 6.1 Hz, 1H, CH); 3.82 (s, 3H, CH_3); 3.72 (s, 3H, CH_3); 2.88 (dd, *J* = 4.4, 16.4 Hz, 1H, CH_2); 2.80 (dd, *J* = 6.1, 16.4 Hz, 1H, CH_2). ^{13}C NMR (100MHz, $CDCl_3$): δ 174.07, 171.18, 67.36, 52.93, 52.28, 38.45.

1. X. Gao, J. Han and L. Wang, *Org. Lett.*, 2015, **B17**, 4596–4599.
2. D. Menche, J. Hassfeld, J. Li, K. Mayer and S. Rudolph, *J. Org. Chem.*, 2009, **74**, 7220-7229.

(2*R,3R)*-(+)-2,3-dihydroxybutanediamide, (2*S*)-(-)-2-hydroxybutanediamide, (±)-2,3-dihydroxybutanediamide, (±)-2-hydroxybutanediamide, (2*R*,3*R*)-(+)-2,3-dihydroxy-*N,N'*-dimethylbutanediamide, (2*S*)-(-)-2-hydroxy-*N,N'*-dimethylbutanediamide, (±)-2,3-dihydroxy-*N,N'*-dimethylbutanediamide, (±)-2-hydroxy-*N,N'*-dimethybutanediamide

The synthetic procedure followed for the synthesis of the enantiopure and racemic primary and methyl amides was adapted from previous procedures[3]. To the appropriate ester (1 equivalent), a solution of an amine (7 N ammonia in methanol or 2.0 M methylamine in THF, 50 equivalents) was added at 0°C over 15 minutes. The reaction flask was fitted with a rubber septum and the contents stirred for 2-3 days to give a colorless solid. The reaction mixture was vacuum filtered and a colorless solid (crystalline or powder) was recovered in 53-93% yield. Crystals viable for X-ray diffraction were obtained by slow evaporation from aqueous or anhydrous MeOH solutions at room temperature.

(2*R,3R)*-(+)-2,3-dihydroxybutanediamide [(+)-2-H]: 93% yield, Mp 197-204 °C. ^{1}H NMR (400 MHz, DMSO-d_6): δ 7.27 (s, 2H, NH_2); 7.15 (s, 2H, NH_2); 5.35 (d, *J* = 7.1 Hz, 2H, OH); 4.17 (d, *J* = 7.3 Hz, 2H, CH). ^{13}C NMR (100 MHz, DMSO-*d*6): δ 175.09, 72.92.

(2*S*)-(-)-2-hydroxybutanediamide [(-)-3-H]: 54% yield, Mp 143-145 °C. ^{1}H NMR (400 MHz, DMSO): δ 7.31 (s, 1H, NH_2); 7.21 (s, 1H, NH_2); 7.14 (s, 1H, NH_2); 6.86 (s, 1H, NH_2); 5.55 (d, *J* = 5.9 Hz, 1H, OH); 4.17 (m, 1H, CH); 2.45 (dd, *J* = 3.4, 14.9 Hz, 1H, CH_2); 2.22 (dd, *J* = 9.5 14.9 Hz, 1H, CH_2). ^{13}C NMR (100 MHz, DMSO-*d*6): δ 176.43, 172.75, 68.86, 40.73.

(±)-2,3-dihydroxybutanediamide [(±)-2-H]: 56% yield, Mp 205 °C (dec). ^{1}H NMR (400 MHz, DMSO): δ 7.27 (s, 2H, NH_2); 7.16 (s, 2H, NH_2); 5.36 (d, *J* = 6.6 Hz, 2H, OH); 4.17 (d, *J* = 6.6 Hz, 2H, CH). ^{13}C NMR (100 MHz, DMSO-*d*6): δ 175.10, 72.93.

(±)-2-hydroxybutanediamide [(±)-3-H]: 74% yield, Mp 156-158 °C. ^{1}H NMR (400 MHz, DMSO): δ 7.32 (s, 1H, NH_2); 7.22 (s, 1H, NH_2); 7.15 (s, 1H, NH_2); 6.87 (s, 1H, NH_2); 5.56 (d, *J* = 5.6 Hz, 1H, OH); 4.18 (m, 1H, CH); 2.45 (dd, *J* = 3.2, 14.9 Hz, 1H, CH_2); 2.23 (dd, *J* = 9.3, 14.9 Hz, 1H, CH_2). ^{13}C NMR (100 MHz, DMSO-*d*6): δ 176.44, 172.77, 68.86, 40.73.

(2*R,3R*)-(+)-2,3-dihydroxy-*N,N'*-dimethylbutanediamide [(+)-2-Me]: 86% yield, Mp 194-195 °C. ^{1}H NMR (400 MHz, DMSO): δ 7.69 (q, *J* = 4.6 Hz, 2H, NH); 5.49 (s, 2H, OH); 4.22 (s, 2H, CH); 2.63 (d, *J* = 4.6 Hz, 6H, CH_3). ^{13}C NMR (100 MHz, DMSO-*d*6): δ 172.97, 72.99, 25.96.

(2*S*)-(-)-2-hydroxy-*N,N'*-dimethylbutanediamide [[(-)-3-Me]]: 87% yield, Mp 67-69 °C. ^{1}H NMR (400 MHz, DMSO): δ 7.79 (m, 2H, NH); 5.70 (br s, 1H, OH); 4.23 (dd, *J* = 3.2, 9.5 Hz, 1H, CH); 2.60 (d, *J* = 4.7 Hz, 3H, CH_3); 2.58 (d, *J* = 4.7 Hz, 3H, CH_3); 2.47 (dd, *J* = 3.2, 14.4 Hz, 1H, CH_2); 2.19 (dd, *J* = 9.5, 14.4 Hz, 1H, CH_2). ^{13}C NMR (100 MHz, DMSO-*d*6): δ 174.22, 170.96, 69.08, 41.17, 25.97, 25.86.

(±)-2,3-dihydroxy-*N,N'*-dimethylbutanediamide [(±)-2-Me]: 85% yield, Mp 167 (dec). ^{1}H NMR (400 MHz, DMSO): δ 7.65 (q, *J* = 4.5 Hz, 2H, NH); 5.46 (s, 2H, OH); 4.21 (s, 2H, CH); 2.58 (d, *J* = 4.5 Hz, 6H, CH_3). ^{13}C NMR (100 MHz, DMSO-*d*6): δ 173.01, 73.06, 26.01.

(±)-2-hydroxy-*N,N'*-dimethybutanediamide [(±)-3-Me]: 62% yield, Mp 153-156 °C. ^{1}H NMR (400 MHz, DMSO): ^{1}H NMR (400 MHz, DMSO): δ 7.78 (m, 2H, NH); 5.69 (s, 1H, OH); 4.23 (m, 1H, CH); 2.60 (d, *J* = 4.7

3. P. F. Frankland and A. Slator, *J. Chem. Soc., Trans.*, 1903, **83**, 1349-1367.

Hz, 3H, CH_3); 2.58 (d, *J* = 4.7 Hz, 3H, CH_3); 2.47 (dd, *J* = 3.4, 14.7 Hz, 1H, CH_2); 2.19 (dd, *J* = 9.5, 14.7 Hz, 1H, CH_2). ^{13}C NMR (100 MHz, DMSO-*d*6): δ 174.20, 170.95, 69.08, 41.17, 25.97, 25.87.

(2*R*,3*R*)-(+)-2,3-dihydroxy-*N,N'*-dibutylbutanediamide, (2*S*)-(-)-2-hydroxy-*N,N'*-dibutylbutanediamide, (±)-2,3-dihydroxy-*N,N'*-dibutylbutanediamide, (±)**-2-hydroxy-*N,N'*-dibutylbutanediamide**

Synthesis of the butylamide compounds was adapted from a previous procedure[4]. A solution of the appropriate ester (1 equivalent), butylamine (4.3 equivalents), and mesitylene (1.3 equivalents) was heated at 170°C and refluxed for 3.5 hours. The excess solvent was removed under *vacuo*, and the resulting solid rinsed with solvent (diethyl ether or EtOAc) to give a colorless solid (crystalline or powder) in 46-90% yield. Crystals viable for X-ray diffraction were obtained by slow evaporation of anhydrous MeOH solutions at room temperature.

(2*R*,3*R*)-(+)-2,3-dihydroxy-*N,N'*-dibutylbutanediamide [(+)-2-Bu]: 90% yield, Mp 186-193 °C. ^{1}H NMR (400 MHz, $CDCl_3$): δ 7.11 (s, 2H, NH); 5.53 (s, 2H, OH); 4.26 (s, 2H, CH); 3.29 (q, *J* = 6.8 Hz, 4H, CH_2); 1.52 (quin, *J* = 7.1 Hz, 4H, CH_2); 1.36 (sex, *J* = 7.3 Hz, 4H, CH_2); 0.94 (t, *J* = 7.3 Hz, 6H, CH_3). ^{13}C NMR (100 MHz, $CDCl_3$): δ 173.92, 70.01, 38.75, 31.38, 19.89, 13.66.

(2*S*)-(-)-2-hydroxy-*N,N'*-dibutylbutanediamide [(-)-3-Bu]: 57% yield, Mp 162-165 °C. ^{1}H NMR (400 MHz, $CDCl_3$): δ 7.05 (s, 1H, NH); 6.11 (s, 1H, NH); 4.36 (m, 1H, CH); 3.27 (m, 4H, CH_2); 2.77 (dd, *J* = 3.4, 15.0 Hz, 1H, CH_2); 2.60 (dd, *J* = 7.0, 15.0 Hz, 1H, CH_2); 1.51 (m, 4H, CH_2); 1.37 (m, 4H, CH_2); 0.94 (t, *J* = 7.3 Hz, 6H, CH_3). ^{13}C NMR (100 MHz, $CDCl_3$): δ 172.47, 172.17, 77.22, 69.45, 39.27, 38.86, 38.26, 31.55, 31.43, 20.01, 13.72, 13.69.

(±)-2,3-dihydroxy-*N,N'*-dibutylbutanediamide [(±)-2-Bu]: 46% yield, Mp 162-165 °C. ^{1}H NMR (400 MHz, DMSO): δ 7.61 (t, *J* = 5.6, 11.7 Hz, 2H, NH); 5.47 (d, *J* = 7.3 Hz, 2H, OH); 4.20 (d, *J* = 7.1 Hz, 2H, CH_2); 3.10 (q, *J* = 6.9 Hz, 4H, CH_2): 1.40 (quin, *J* = 7.1 Hz, 4H, CH_2); 1.27 (sex, *J* = 7.6 Hz, 4H, CH_2); 0.87 (t, *J* = 7.3 Hz, 6H, CH_3). ^{13}C NMR (100 MHz, DMSO-*d*6): δ 172.29, 72.97, 38.49, 31.78, 19.94, 14.18.

4. B. A. Shainyan, M. V. Ustinov, V. K. Belśkii and L. O. Nindakova, *Russ. J. Org. Chem.*, 2002, **38**, 104-110.

S2. X-ray Crystallography

Crystallography. Crystallographic details for compounds (+)-**2**-H/(-)-**3**-H, (±)-**2**-H, (±)-**3**-H, (+)-**2**-Me/(-)-**3**-Me, (±)-**2**-Me, (±)-**3**-Me, (+)-**2**-Bu/(-)-**3**-Bu and (±)-**2**-H are summarized in Table S1. X-ray data were collected on a Bruker APEX II CCD diffractometer using phi and omega scans with graphite monochromatic Cu Mo $K\alpha$ (λ = 1.54178 Å) radiation. Data sets were corrected for Lorentz and polarization effects as well as absorption. The criterion for observed reflections is $I > 2\sigma(I)$. Lattice parameters were determined from least-squares analysis and reflection data. Empirical absorption corrections were applied using SADABS.[5] Structures were solved by direct methods and refined by full-matrix least-squares analysis on F^2 using X-SEED[6] equipped with SHELXS[7]. All non-hydrogen atoms were refined anisotropically by full-matrix least-squares on F^2 by the use of the SHELXL[8] program. H atoms (for OH and NH) were located in difference Fourier synthesis and refined isotropically with independent O/N-H distances or restrained to 0.85(2) Å. The remaining H atoms were included in idealized geometric positions with U_{iso}=1.2U_{eq} of the atom to which they were attached (U_{iso}=1.5U_{eq} for methyl groups). Molecular configurations were compared to both the known chirality of the tartaramide and malamide components and estimated Flack parameters[9] and where applicable, atomic coordinates were inverted to achieve correct structural configurations.

5. G. M. Sheldrick, SADABS and TWINABS—Program for Area Detector Absorption Corrections, University of Göttingen, Göttingen, Germany, 2010.
6. L. J. Barbour, *J. Supramol. Chem.*, 2001, **1**, 189.
7. G. M. Sheldrick, *Acta Crystallogr., Sect. A: Fundam. Crystallogr.*, 2008, **64**, 112.
8. G. M. Sheldrick, *Acta Crystallogr., Sect. C: Struct. Chem.*, 2015, **71**, 3-8.
9. H. D. Flack, *Acta Crystallogr.*, **1983**, *39,* 876-881.

Table S1. Crystallographic data.

	(+)-**2**-H/(-)-**3**-H	(±)-**2**-H	(±)-**3**-H
Crystal data			
CCDC deposit no.	1832191	1832194	1832192
Empirical formula	$C_8H_{16}N_4O_7$	$C_4H_8N_2O_4$	$C_4H_8N_2O_3$
Crystal System, space group	monoclinic $P2_1$	monoclinic $P2_1/c$	monoclinic $P2_1/c$
M_r	280.25	148.12	132.12
a, Å	8.0233(5)	8.0175(4)	9.4044(2)
b, Å	7.9864(6)	8.1062(4)	8.2033(2)
c, Å	9.3673(6)	9.2562(4)	7.7750(2)
α, deg	90	90	90
β, deg	95.686(2)	95.619(2)	101.659(1)
γ, deg	90	90	90
V, (Å^3)	597.28(7)	598.68(5)	587.44(2)
Z, Z'	2, 1	4, 1	4, 1
D_{calc} (g cm^{-3})	1.558	1.643	1.494
μ, (Mo Kα) (mm^{-1})	1.189	1.287	1.105
F_{000}	296	312	280
temp (K)	100(2)	100(2)	100(2)
Crystal form, color	plate, colorless	block, colorless	block, colorless
Crystal size, mm	0.42 x 0.28 x 0.11	0.40 x 0.34 x 0.20	0.27 x 0.27 x 0.4
Data collection			
Diffractometer	Bruker Apex II	Bruker Apex II	Bruker Apex II
T_{min}/ T_{max}	0.633/0.876	0.630/0.783	0.739/0.860
No. of refls. (meas., uniq., and obs.)	8907/2042/2022	8705/1082/1067	8515/1067/1049
R_{int}	0.0239	0.0292	0.0227
ϑ_{max} (°)	68.209	68.228	68.209
Refinement			
$R/R^2{}_\omega$ (obs data)	0.282/0.0752	0.0330/0.0857	0.0329/0.0882
$R/R^2{}_\omega$ (all data)	0.284/0.0756	0.0333/0.0860	0.0332/0.0885
S	1.07	1.18	1.01
No. of refls.	2042	1082	1067
No. of parameters	225	109	97
$\Delta\rho_{max/min}$ (e·Å^{-3})	0.186/-0.342	0.275/-0.314	0.457/-0.251
Flack	-0.02(7)	-	-

Table S1. Crystallographic data (continued).

	(+)-**2**-Me/(-)-**3**-Me	(±)-**2**-Met	(±)-**3**-Met
Crystal data			
CCDC deposit no.	1832193	1832196	1832197
Empirical formula	$C_{12}H_{24}N_4O_7$	$C_6H_{12}N_2O_4$	$C_6H_{12}N_2O_3$
Crystal System, space group	Triclinic, *P*1	orthorhombic *Pccn*	monoclinic $P2_1/c$
M_r	336.35	176.18	160.18
a, Å	5.0193(30	9.8954(4)	19.637(4)
b, Å	8.6051(6)	19.3100(9)	4.9347(13)
c, Å	10.2069(7)	8.9868(4)	8.4645(17)
α, deg	69.005(4)	90	90
β, deg	77.721(4)	90	92.281(12)
γ, deg	89.513(4)	90	90
V, (Å^3)	401.06(5)	1717.20(13)	819.6(3)
Z, *Z'*	1, 1	8, 1	4, 1
D_{calc} (g cm^{-3})	1.393	1.363	1.298
μ, (Mo Kα) (mm^{-1})	0.976	0.983	0.881
F_{000}	180	752	344
temp (K)	100(2)	100(2)	100(2)
Crystal form, color	plate, colorless	needle, colorless	plate, colorless
Crystal size, mm	0.41 x 0.39 x 0.08	0.29 x 0.10 x 0.05	0.36 x 0.21 x 0.05
Data collection			
Diffractometer	Bruker Apex II	Bruker Apex II	Bruker Apex II
T_{min}/ T_{max}	0.538/0.753	0.762/0.953	0.741/0.956
No. of refls. (meas., uniq., and obs.)	8655/2517/2467	24009/1570/1318	10151/1369/1122
R_{int}	0.372	0.0622	0.0783
ϑ_{max} (°)	68.234	68.19	65.06
Refinement			
R/R^2_ω (obs data)	0.0389/0.0960	0.0371/0.0996	0.0628/0.1894
R/R^2_ω (all data)	0.0394/0.0968	0.0455/0.1060	0.0734/0.2231
S	1.04	1.02	1.14
No. of refls.	2517	1570	1369
No. of parameters	240	127	114
$\Delta\rho_{max/min}$ (e·Å^{-3})	0.322/-0.189	0.289/-0.367	0.342/-0.390
Flack	-0.03(10)	-	-

Table S1. Crystallographic (continued).

	(+)-**2**-Bu/(-)-**3**-Bu	(±)-**2**-Bu
Crystal data		
CCDC deposit no.	1832198	1832195
Empirical formula	$C_{24}H_{48}N_4O_7$	$C_{12}H_{24}N_2O_4$
Crystal System, space group	triclinic *P*1	Monoclinic, *C*2/*c*
M_r	504.66	260.33
a, Å	4.9064(3)	31.8791(12)
b, Å	8.7118(6)	5.0676(2)
c, Å	17.1527(14)	8.8564(4)
α, deg	102.543(7)	90
β, deg	96.249(5)	96.049(4)
γ, deg	90.472(5)	90
V, (Å^3)	711.03(9)	1422.79(10)
Z, *Z'*	1, 1	4, 1
D_{calc} (g cm^{-3})	1.179	1.215
μ, (Mo Kα) (mm^{-1})	0.704	0.747
F_{000}	276	568
temp (K)	100(2)	100(2)
Crystal form, color	plate, colorless	plate, colorless
Crystal size, mm	0.20 x 0.14 x 0.03	0.33 x 0.13 x 0.11
Data collection		
Diffractometer	Bruker Apex II	Bruker Apex II
T_{min}/T_{max}	0.872/0.979	0.793/0.922
No. of refls. (meas., uniq., and obs.)	15213/4727/4188	14676/1307/1211
R_{int}	0.0365	0.0380
ϑ_{max} (°)	68.17	68.116
Refinement		
$R/R^2{}_\omega$ (obs data)	0.0453/0.1155	0.0435/0.1163
$R/R^2{}_\omega$ (all data)	0.0528/0.1207	0.0460/0.1188
S	1.05	1.09
No. of refls.	4727	1307
No. of parameters	323	89
$\Delta\rho_{max/min}$ (e·Å^{-3})	0.258/-0.174	0.362/-0.155
Flack	0.16(10)	-

S3. Hydrogen-Bond Tables

Table S2 Hydrogen Bond Geometries

Compound	D-H···A (Å)	D···A (Å)	D-H···A (°)	Symmetry operator
(+)-**2**-H/(-)-**3**-H	N1A-H···O1B	2.862(2)	146(2)	*1-x, y+1/2, 1-z*
	N1A-H···O4A	2.857(2)	173(3))	*1+x, y, z*
	N2A-H···O2B	2.996(2)	171(3)	*1-x, y+1/2, 2-z*
	N2A-H···O3A	2.969(3)	134(3)	*-x, y-1/2, 2-z*
	N1B-H···O3B	2.851(2)	174(3)	*x-1, y, z*
	N1B-H···O1A	2.876(3)	143(2)	*1-x, y-1/2, 2-z*
	N2B-H···O2A	2.973(2)	167(3)	*1-x, y-1/2, 1-z*
	N2B-H···O1B	3.347(2)	150(3)	*1+x, y, z*
	O2A-H···O1A	2.670(2)	173(3)	*1-x, y-1/2, 2-z*
	O2B-H···O1B	2.719(3)	166(3)	*1 -x, y+1/2, 1-z*
	O3A-H···O3B	2.753(2)	132(3)	*x-1, 1+y, z*
(±)-**2**-H	N1-H···O2	3.0453(14)	137.1(15)	*-x, y-1/2, -z+1/2*
	N1-H···O3	2.9775(15)	169.9(16)	*x, -y+1/2, z+1/2*
	N2-H···O4	2.8951(15)	145.0(14)	*x, -y+1/2, z-1/2*
	N2-H···O1	2.9083(14)	175.8(16)	*1+x, y, z*
	O2-H···O1	2.8181(13)	136.5(15)	*-x, 1-y, -z*
	O3-H···O4	2.6690(13)	174.1(17)	*1-x, y-1/2, -z+1/2*
(±)-**3**-H	N1 O1	2.9740(15)	150.3(15)	*1-x, y+1/2, -z+1/2*
	N1 O2	2.9411(15)	160.8(16)	*1-x, y-1/2, -z+1/2*
	N2 O1	2.8623(14)	168.7(15)	*2-x, y+1/2, -z+1/2*
	N2 O3	2.8844(14)	169.8(16)	*2-x, y-1/2, -z+1/2*
	O2 O3	2.6791(13)	173.0(16)	*x, -y+1/2, z+1/2*
(+)-**2**-Me/(-)-**2**-Me	N1A-H···O1B	3.080(3)	158(4)	*x-1, y, z*
	N2A-H···O4A	2.790(3)	146(3)	*x-1, y, z*
	N1B-H···O1A	3.112(3)	154(4)	*x+1, y-1, z*
	N2B-H···O3B	2.897(3)	173(4)	*x+1, y, z*
	O2A-H···O1B	2.758(2)	172(4)	*x, y, z*
	O3A-H···O2B	2.742(2)	157(4)	*x-1, y+1, z*
	O2B-H···O1A	2.668(3)	173(4)	*x, y-1, z*
(±)-**2**-Me	N1-H···O1	2.8985(18)	150(2)	*x, -y+1/2, z-1/2*
	N2-H···O3	2.9562(19)	137.2(19)	*1-x, 1-y, -z*
	O2-H···O1	2.7527(17)	169(3)	*-x+3/2, y, z-1/2*
	O3-H···O4	2.6646(17)	173(3)	*x-1/2, 1-y, -z+1/2*
(±)-**3**-Me	N1-H···O1	3.015(3)	157(4)	*x, -y+1/2, z-1/2*
	N2-H···O3	2.862(3)	177(5)	*x, y-1, z*
	O2-H···O1	2.740(3)	171(4)	*x, -y+3/2, z-1/2*
(+)-**2**-Bu/(-)-**3**-Bu	N1A-H···O1A	2.730(4)	150(5)	*x-1, y, z*
	N2A-H···O1B	3.194(4)	168(4)	*x-1, 1+y, z*
	O2A-H···O2B	2.725(4)	159(4)	*x-1, y, z*
	O3A-H···O1B	2.736(4)	159(5)	*x, 1+y, z*
	N1B-H···O4A	3.233(4)	163(4)	*1+x, y, z*
	N2B-H···O4B	2.891(4)	177(5)	*1+x, y, z*
	O2B-H···O4A	2.673(4)	171(5)	*x, y, z*
(±)-**2**-Bu	N1-H···O1	2.907(2)	134(2)	*x, y-1, z*
	O2-H···O1	2.787(2)	165(2)	*x, 1-y, z+1/2*

S4. Computational Methods and Results

Density Functional Theory

Experimental crystal structure optimizations. All experimental crystal structures were optimized using plane-wave-based periodic DFT using the VASP[10][11][12][13] package. Structural optimization was performed in two steps to aid convergence -- an initial optimization in which only atomic positions were optimized (i.e. the lattice parameters were held fixed at experimental values) followed by a second optimization in which both atomic positions and cell parameters are fully flexible. Throughout our calculations, the PBE exchange-correlation functional was employed, supplemented with the Becke-Johnson-damped Grimme D3 (GD3BJ) dispersion correction. All calculations made use of the projector-augmented wave (PAW) method[14] and the standard supplied pseudopotentials[15]. The following geometry optimization convergence criteria were used for all calculations: a plane-wave energy cutoff of 500 eV, an energy tolerance in convergence of the electronic minimization of 1×10^{-7} eV per atom, and a force tolerance in the geometry optimization of 3×10^{-2} eV Å^{-1}.

Single molecule calculations. To be consistent with the periodic crystal structure calculations, single molecule energies were calculated using VASP and the same computational settings used for crystal structure calculations. Molecular geometries were extracted from the final, geometry optimized experimental crystal structures and placed in a cubic unit cell with cell lengths of 50 Å. This size was chosen as large enough that molecules do not interact with their periodic images. Single point energies were calculated, followed by geometry optimization of all atomic coordinates (with the unit cell fixed).

The lattice energy was calculated as the total energy of the geometry optimized crystal structure minus the energy of the lowest energy geometry optimized conformation of the constituent isolated molecules; no conformer prediction was performed, but we took the lowest energy of all instances of each molecule from all experimental crystal structures.

The intermolecular energy of each crystal structure was calculated as the total energy of the geometry optimized crystal structure minus the single-point energy of the isolated molecules in the geometry found in the optimized crystal structure.

The strain energy of each molecule in each crystal structure was calculated as the difference in energy between the single-point energy of the isolated molecules in the geometry found in the optimized crystal structure and the energy of the geometry optimized molecule, starting from the geometry in that crystal structure.

The conformational energy of each molecule in each crystal structure was calculated as the difference in energy between the single-point energy of the isolated molecules in the geometry found in the optimized crystal structure and the energy of the lowest energy geometry optimized version of each molecule, considering all molecular geometries of that molecule in all observed crystal structures.

10. G. Kresse and J. Hafner, *Phys. Rev. B: Condens. Matter Mater. Phys*., 1993, **47**, 558–561.
11. G. Kresse and J. Hafner, *Phys. Rev. B: Condens. Matter Mater. Phys.*, 1994, **49**, 14251–14269.
12. G. Kresse and J. Furthmüller, *Comput. Mater. Sci.* 1996, **6**, 15–50.
13. G. Kresse and J. Furthmüller, *Phys. Rev. B: Condens. Matter Mater. Phys*. 1996, **54**, 11169–11186.
14. P.E. Blöchl, *Phys. Rev. B: Condens. Matter Mater. Phys*., 1994, *50*, 17953–17979.
15. G. Kresse and D. Joubert, *Phys. Rev. B: Condens. Matter Mater. Phys*. 1999, **59**, 1758–1775

Hypothetical crystal structure optimizations. Hypothetical quasiracemic crystal structures were created for the (+)-**2**-Me/(-)-**3**-Me and (+)-**2**-Bu/(-)-**3**-Bu systems by modification of the experimentally determined racemic (±)-**2**-Me, (±)-**3**-Me and (±)-**3**-Bu crystal structures.

(±)-**2**-Me was converted to two hypothetical (+)-**2**-Me/(-)-**3**-Me quasiracemates by replacing an OH group on the (-)-**2**-Me molecule with an H. Two options of which OH group to replace led to two possible quasiracemates with approximate inversion symmetry. We label these two structures as hypothetical quasiracemates A and B.

Two hypothetical quasiracemates (labelled C and D) with approximate inversion symmetry were also created from the observed (±)-**3**-Me crystal structure by modifying an H atom to an OH group. In this case, only one H atom can be modified to create a Me-tartaramide molecule of the correct stereochemistry to form a quasiracemate. However, there is still freedom in where to orient the hydrogen atom of the newly created OH group and two sensible orientations can be achieved, with the OH group forming an intermolecular hydrogen bond. In structure C, this hydrogen bond is formed with an amide oxygen of a neighboring molecule, while in structure D, the new hydrogen bond is formed with the oxygen atom of a hydroxyl group on a neighboring molecule. The structures are shown in Figure S1.

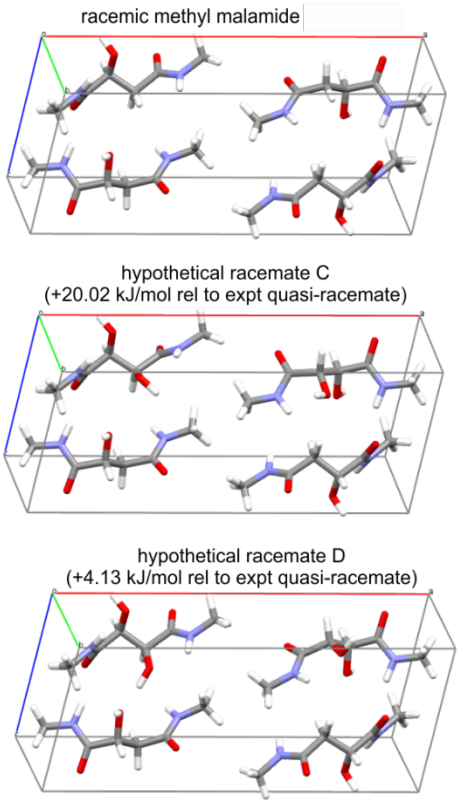

Figure S1. Packing of hypothetical quasiracemates C and D created by mutation of one of the Me-malamide molecules in the experimentally determined racemate (top).

After geometry optimization, using the same computational settings used for the experimentally determined crystal structures, the energies of these four hypothetical quasiracemates relative to the observed quasiracemate (+)-**2**-Me/(-)-**3**-Me were: +29.62 kJ mol^{-1} (structure A); +9.07 kJ mol^{-1} (structure

B); +20.02 kJ mol^{-1} (structure C) and +4.13 kJ mol^{-1} (structure D), all per pair of quasienantiomeric molecules.

A similar procedure was used to create two hypothetical quasiracemates of (+)-**2**-Bu/(-)-**3**-Bu from (±)-**2**-Bu, creating hypothetical structures E and F, whose calculated energies are 22.90 (structure E) and 23.19 kJ mol^{-1} above the energy of the experimentally determined quasiracemate (+)-**2**-Bu/(-)-**3**-Bu.

The structures of these six hypothetical structures are provided as part of the supplementary information.

Crystal Explorer

Crystal structure files of (±)-**2**-H, (±)-**3**-H, and (+)-**2**-H/(-)-**3**-H were used as input for Crystal Explorer[16]. Hirschfield surfaces were calculated for each component at the *high accuracy* level" for electron density under B3LYP/6-31G(d,p) in Tonto. Molecular clusters were prepared by completing fragments within 3.5 Å of a single reference molecule and those fragments that lacked hydrogen bond connectivity to the original reference molecule were removed. For quasiracemate (+)-**2**-H/(-)-**3**-H, two separate calculations were performed using the (+)-**2**-H or (-)-**3**-H as the reference molecule. Interaction energy calculations of the central molecule were performed using B3LYP/6-31G(d,p) in Tonto and the calculated energy was partitioned (*i.e.*, electrostatic, polarization, dispersion, and exchange-repulsion) and weighted for total energy determination as prescribed by Crystal Explorer for Tonto (Table S3). The energy components for each compound were compared and identified as illustrated in Figure S2 for (±)-**3**-H. Total summed energies of -389.4, -378.2, -371.0, and -331.6 kJ mol^{-1} were determined for (±)-**3**-H, (+)-**2**-H/(-)-**3**-H [(+)-**2**-H reference molecule], (+)-**2**-H/(-)-**3**-H [(-)-**3**-H reference molecule], and (±)-**2**-H, respectively.

Table S3 Calculated Lattice Interaction Energies.

Interaction Identity	Symmetry Operation	Radius (Å)	E_{ele} (kJ/mol)	E_{pol} (kJ/mol)	E_{dis} (kJ/mol)	E_{rep} (kJ/mol)	E_{tot} (kJ/mol)
(±)-**3**-H							
A, B	x,y,z	8.02	-45.1	-10.6	-10.8	39.3	-40.7
C	-x,-y,-z	6.32	-10.8	-2.8	-10.3	4.5	-19.7
D	-x,-y,-z	6.16	-24.1	-7.0	-10.2	34.5	-18.3
E, F	-x, y+1/2, -z+1/2	5.96	-15.6	-4.1	-16.4	15.0	-24.5
G, H	-x, y+1/2, -z+1/2	5.50	-50.2	-15.1	-21.2	74.3	-36.8
I	-x, -y+1/2, -z+1/2	4.89	-70.1	-17.1	-26.9	59.0	-73.7
J	-x, -y+1/2, -z+1/2	4.89	-70.1	-17.1	-26.9	59.0	-73.7
(+)-**2**-H/(-)-**3**-H [(+)-**2**-H as reference molecule]							
A, B	x,y,z	8.02	-56.6	-12.8	-10.3	47.7	-48.8
C	pseudo -x,-y,-z	6.52	-7.6	-1.9	-7.6	2.6	-14.5
D	pseudo -x,-y,-z	6.27	-12.7	-6.5	-7.5	20.3	-12.2
E, F	-x, y+1/2, -z+1/2	5.88	-4.3	-3.4	-14.6	5.6	-16.4
G, H	-x, y+1/2, -z+1/2	5.47	-47.5	-12.4	-18.5	58.7	-39.3
I	pseudo -x, -y+1/2, -z+1/2	4.97	-68.5	-17.9	-24.1	55.7	-72.3

16. M. A. Spackman and D. Jayatilaka, *CrystEngComm*, 2009, **11**, 19.

J	pseudo -x, -y+1/2, -z+1/2	4.75	-70.1	-16.2	-25.9	62.2	-70.2
(+)-**2**-H/(-)-**3**-H [(-)-**3**-H as reference molecule]							
A, B	x,y,z	8.02	-48.2	-11.1	-10.8	46.0	-40.1
C	pseudo -x,-y,-z	6.52	-7.6	-1.9	-7.6	2.6	-14.5
D	pseudo -x,-y,-z	6.27	-12.7	-6.5	-7.5	20.3	-12.2
E, F	-x, y+1/2, -z+1/2	5.87	-16.4	-4.2	-17.9	19.6	-24.0
G, H	-x, y+1/2, -z+1/2	5.52	-50.0	-15.0	-21.1	73.6	-36.8
I	pseudo -x, -y+1/2, -z+1/2	4.97	-68.5	-17.9	-24.1	55.7	-72.3
J	pseudo -x, -y+1/2, -z+1/2	4.75	-70.1	-16.2	-25.9	62.2	-70.2
(±)-**2**-H							
K, L	-x, y+1/2, -z+1/2	6.67	-51.9	-10.2	-12.7	45.4	-45.4
M, N	-x, y+1/2, -z+1/2	5.85	-84.6	-22.1	-19.3	78.8	-73.9
O, P	x, -y+1/2, z+1/2	5.67	-60.2	-16.7	-12.3	65.2	-46.5

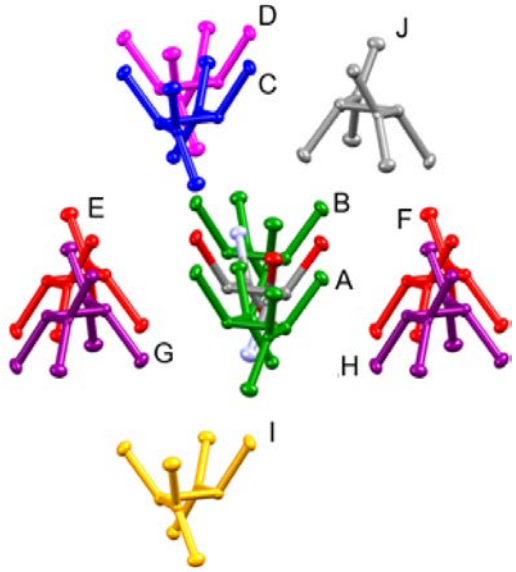

Figure S2. Cluster analysis scheme for (±)-**3**-H showing central reference molecule and neighboring molecular interaction components

S5. Differential Scanning Calorimetry

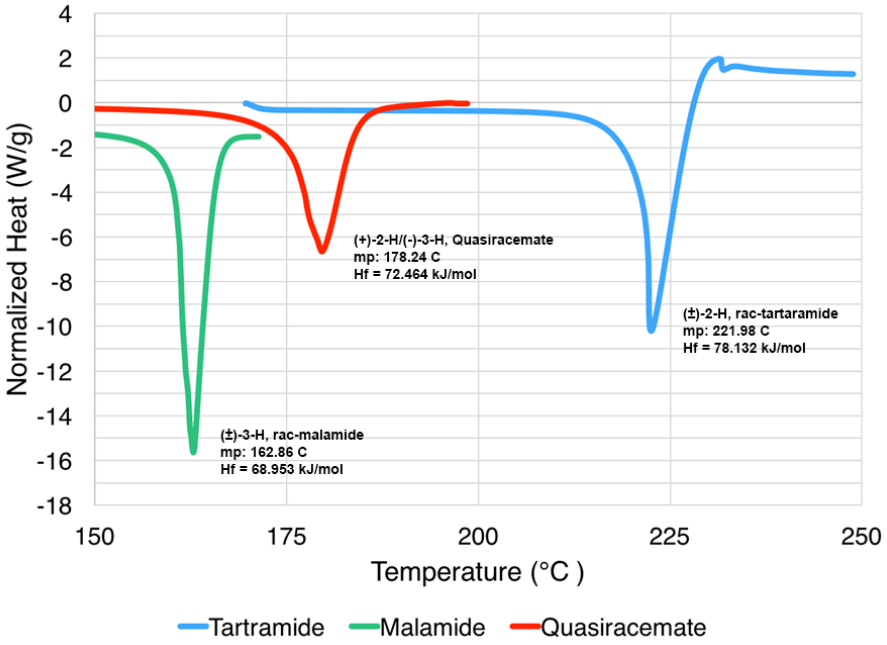

DSC experiments were carried out on a TA DSC-25 using sealed aluminum Tzero pans. All samples were processed with a 10 °C/min ramp rate and dry N_2 purge gas. No cooling curves were produced due to decomposition of samples upon heating above – this decomposition was especially noticeable for (±)-**3**-H at temperatures above the melting point. Thermodynamic data provided below were calculated for each racemic and quasiracemic pair of molecules.

Property	(±)-**2**-H	(±)-**3**-H	(+)-**2**-H/(-)-**3**-H
Melting Point (°C)	221.98	162.86	178.24
H_f (J g^{-1})	263.75	260.95	258.58
H_f (kJ mol^{-1})	78.132	68.953	72.464